18th International Conference
ENGINEERING MECHANICS 2012
Svratka, Czech Republic, May 14 – 17, 2012

pp. 1497–1504
Paper #186

NUMERICAL PREDICTION OF PARASITIC ENERGY DISSIPATION IN WEDGE SPLITTING TESTS ON CONCRETE SPECIMENS

V. Veselý[*], T. Holušová[**], S. Seitl[***]

Abstract: *Undesirable energy dissipation taking place during wedge-splitting tests on cementitious composites and resulting in overestimation of the values of the determined fracture-mechanical characteristics of the tested materials is investigated in this paper via numerical simulations performed using a commercial finite element method tool with an implemented cohesive crack model. The rather broad range of cohesive behaviour of the studied materials was simulated through adjustments made to the corresponding characteristic length of the composite. The parasitic amount of energy is dissipated in fracture processes around the corners of the groove for the insertion of the loading platens, as these corners introduce rather strong stress concentrators to the specimen. This amount was extracted from simulated load-displacement curves and it was discovered that the amount considerably depends on the specimen proportions but its dependence on the level of material brittleness is not so significant.*

Keywords: ***wedge-splitting test, concrete fracture, specimen proportions, energy dissipation, numerical simulation***

1. Introduction

The wedge splitting test can be conveniently used for measuring the fracture-mechanical parameters of quasi-brittle building materials, particularly cement-based composites. The desirable failure propagation in the area of the ligament of the test specimen, i.e. starting at the specimen's notch tip and propagating towards the opposite surface of the specimen, can be accompanied by parasitic failure around the other considerable stress concentrator(s) – the corner(s) of the groove for inserting the loading platens. The amount of energy released in such failures is not being separated from the energy consumed in the desired fracture process within ordinary testing and evaluation procedures. Therefore, noticeable errors in the values of fracture parameters may arise in some cases depending on the specimen's proportions and the test configuration. The paper presents the results of a numerical study conducted in order to develop and propose a solution applicable in the evaluation of classical fracture-mechanical parameters via the wedge-splitting test, which in this case was carried out on cylinder-shaped specimens prepared either as standard test specimens cast into cylinder moulds or as cores drilled from existing structures by a hollow drill. This numerical study will be accompanied by experimental validation; however, the experimental campaign is not finished yet, so only the results of the numerical part of the study are presented in the paper. The experimental data from a rather broad test series (under preparation) will be evaluated using the proposed procedure stemming from the results of the numerical simulations.

2. Wedge-splitting test configuration

The test referred to as the wedge-splitting test is considered in this paper. A variety of notched specimen shapes can be used with it; see Fig. 1 or (Linsbauer & Tschegg, 1986, Brühwiler & Wittmann, 1990). This work is exclusively focused on cylinder-shaped specimens with a diameter of 150 mm and a width of 100 mm. The paper presents selected results from work by Holušová (2012). A similar analysis was also carried out by the authors for cube-shaped (or square-prism-

· Ing. Václav Veselý, Ph.D.: Brno University of Technology, Faculty of Civil Engineering, Institute of Structural Mechanics, Veveří 331/95; 602 00, Brno; CZ, e-mail: vesely.v1@fce.vutbr.cz

·[*] Ing. Táňa Holušová: ditto, e-mail:holusova.t@ fce.vutbr.cz

·[**] Ing. Stanislav Seitl, Ph.D.: Academy of Sciences of the Czech Republic, v. v. i., Institute of Physics of Materials; Žižkova 22; 616 62, Brno; CZ, e-mail: seitl@ipm.cz

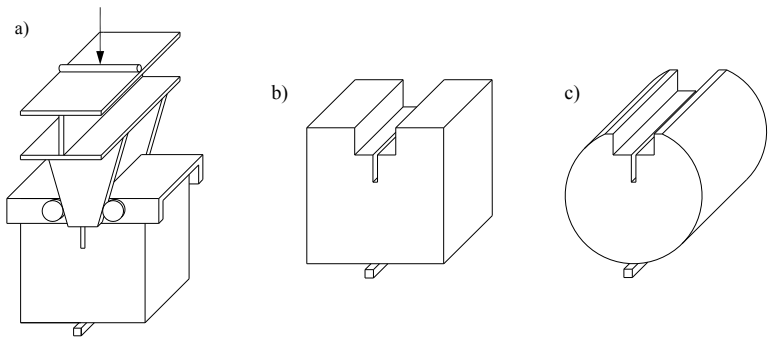

Fig. 1: Wedge splitting test configuration: schematic diagrams of the loading mechanism (a) and typical specimen shapes (b, c) (adapted from Brühwiler & Wittmann, 1990)

shaped) WST specimens (Řoutil et al., 2010, 2011a,b, 2012, Veselý et al., 2011). The wedge-splitting test configuration is becoming frequently used in the area of quasi-brittle materials and related fields connected with numerical modelling, inverse analysis, material research, etc.

3. Problem description

The studied problematic aspect of the WST concerns the area in the upper part of the specimen where the load is imposed. Apart from the main stress concentrator – the notch tip – the specimen includes other two stress concentrators – the corners of the groove for inserting the loading platens. For the correct evaluation of the fracture experiment, the failure should only take place between the initial notch tip and the specimen's back face (Fig. 2 left). In the case of quasi-brittle materials, which are characterized by the formation of what is referred to as a fracture process zone (FPZ) around the stress concentrator before the macro-crack starts to propagate, the failure can take place at several points in the specimen simultaneously (Fig. 2 middle). A major crack can finally localize in the ligament area, but substantial (undesirable) damage may also occur elsewhere. The occurrence of this failure mode is here considered as the most undesirable during a real test because an unknown amount of energy is released in the failure around the groove corners. If the major crack localizes from the corner (Fig. 2 right), the results of such a test are useless; however, it doesn't lead to an overestimation of the fracture parameters at least, because such a record is not used in the evaluation procedure.

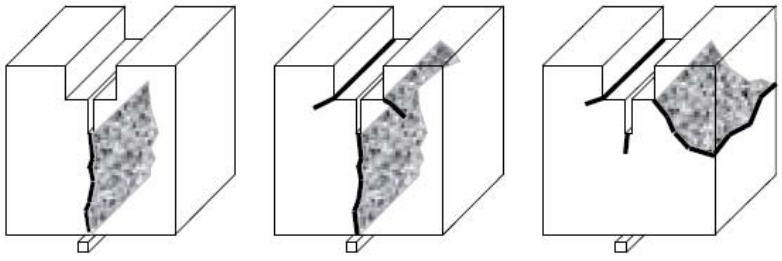

Figure 2: Desirable (left) and undesirable (middle, right) types of failure of the WST specimen (Veselý et al. 2011)

The amount of mechanical energy dissipated in the undesirable failure processes around the groove corners (including potential crushing around the support and loading platens) can be quantified based on the difference between the work of fracture (RILEM, 1985) in the desirable and undesirable failure mode cases. Therefore, two variants of the model for each studied specimen of different proportions were prepared: *i)* a reference variant with the constitutive model for quasi-brittle material used throughout the entire specimen volume (marked as *V1*), and *ii)* an artificial variant with elastic material around the groove corners (marked as *V2*). The differences between the two models are indicated in Fig. 3 left.

The subtraction of the areas under the load–displacement curves corresponding to the reference and alternative model gives an estimation of the amount of energy dissipated in the failure around the groove corners. The loading curve corresponding to the original model typically differs from the

alternative one by the rather wide hump around and after its peak indicating the extra energy release taking place around the corners of the groove for the insertion of the loading platens.

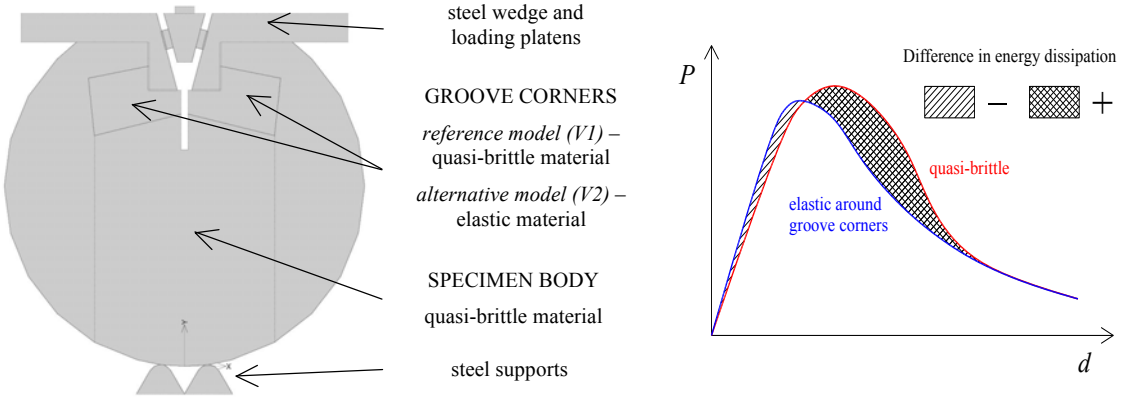

Fig. 3: Illustration of both the reference and alternative geometric model (left); sketch of the evaluation of energy dissipated in failure around the groove corners (right) (Řoutil et al. 2011b)

4. Numerical simulations

The numerical study was conducted using a commercial finite element (FE) tool with an implemented cohesive crack model governing the tensile failure – ATENA 2D software (Červenka et al., 2005).

4.1. Geometrical model, FE mesh

The 2D model used for the study is depicted in Fig. 3 left, where its macroelement structure is outlined, and Fig. 4 right, where the FE mesh and boundary conditions are indicated. The specimen is supported by two closely placed steel supports and loaded via steel angular platens which are being split by a wedge (in 3D reality with the use of roller bearings, in the used 2D model via sliding pads). In the loading groove a no-tension interface is assumed between the concrete specimen and the steel loading platens. The model reflects the boundary condition details of real tests which are currently in preparation (test configuration sketched in Fig. 4 left).

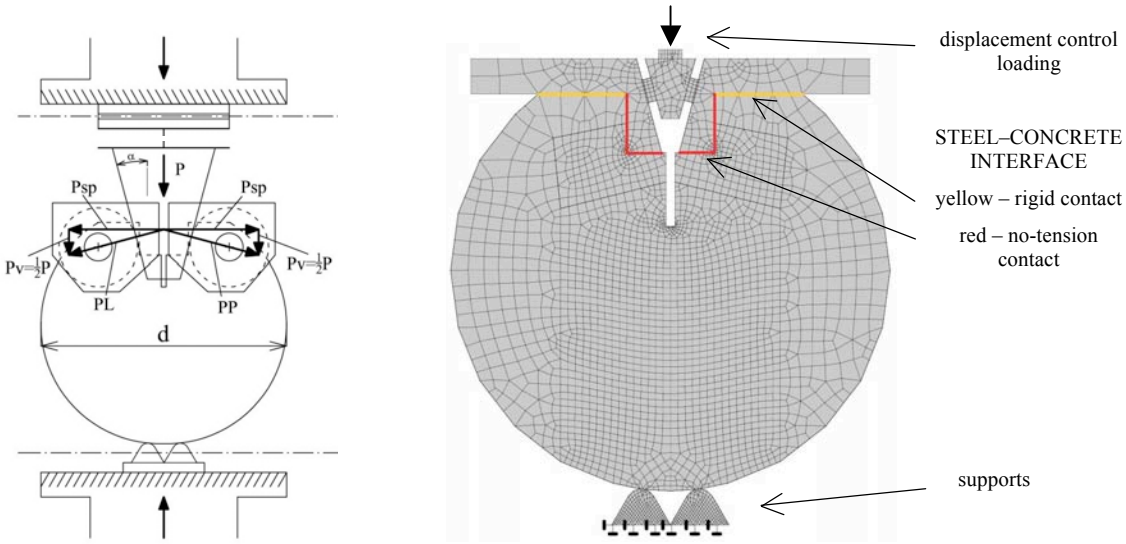

Fig. 4: Considered test configuration with indication of load transfer (left) (Holušová, 2012), FE model with indication of boundary conditions

The model was created in variants with different relative notch lengths α defined as the absolute notch length a (measured as the vertical distance between the roller bearing axis and the notch tip) divided by the specimen width W (measured as the vertical distance between the roller bearing axis and the opposite surface of the specimen). Note that the diameter d of the cylinder-shaped specimen was equal to 150 mm, the height of the segment cut from the top of the specimen was equal to 15 mm, and the distance of the roller bearing axis from the top (flat) surface was 15 mm, so that the specimen

Tab. 1: Modelled notch length variants

a [mm]	7.2	9.6	12	15	18	24	30
α [-]	0.06	0.08	0.1	0.125	0.15	0.2	0.25

width $W = 120$ mm. The values of the notch length a and corresponding relative notch length α are summarized in Tab. 1. The width and depth of the groove for inserting the loading platens is 30 and 20 mm, respectively.

4.2. Material model description

For modelling of the cementitious composite material of the specimen a fracture-plastic material model was used (Červenka et al., 2005); within the employed ATENA software the material model is referred to as the 3D Non Linear Cementitious 2 model. Several material sets were created in order to simulate cementitious composites of a relative wide range of material (quasi-)brittleness, i.e. ranging from rather ductile softening composites (for instance those reinforced with fibres) to nearly brittle ones (for instance cement pastes). For the reference material set (marked *C0*) the default setting of the software for cubic compressive strength $f_{cu} = 35$ MPa was used. The fracture behaviour of the model is governed by the cohesive crack model, which is based on following characteristics: the value of the tensile strength f_t, the shape of the traction–separation law $\sigma(w)$ and the value of fracture energy G_f. The f_t and G_f values of the reference material set were equal to 2.568 MPa and 64.2 Jm^{-2}, respectively. These characteristics, together with a Young's modulus value of $E = 32.29$ GPa, can be linked to a measure of material brittleness via what is referred to as the characteristic length l_{ch}, defined as

$$l_{ch} = \frac{EG_f}{f_t^2}. \tag{1}$$

Hordijk's exponential softening function (Červenka et al., 2005) was used as the traction–separation law. The other material sets used differed from the reference set marked as *C0* in their f_t and G_f values, which were changed in such a way that the reference characteristic length value ${}^0l_{ch}$ was multiplied by the factor 2^{2j}, where $j \in \langle -4,-3,-2,-1,0,1,2 \rangle$. This was obtained by multiplying the ${}^0f_t$ value by $\sqrt{2^j}$ and dividing the value of ${}^0G_f$ by 2^j. The material sets were then marked with the symbol *C*, the value of the multiplying factor $2^{2|j|}$ and a positive or negative sign indicating the increasing or decreasing of the characteristic length value. The corresponding values of the fracture-mechanical parameters entering the computations are shown in Tab. 2; however, only for the non-negative values of j, which mean the increasing of the characteristic length of the reference concrete, i.e. the decreasing of its brittleness. The reason is that for characteristic length values lower than ${}^0l_{ch}$ the results of the present study were found to be of a low significance (Holušová, 2012). On the other hand, the material sets $C2^{2|j|}-$ were used for an analysis leading to the determination of the minimal notch length for major failure propagation from its tip, not the groove corner (details in Holušová, 2012).

Note that the described types of analyses were invented, developed and successively presented in Řoutil et al. (2010a,b), Řoutil et al. (2011a,b), Veselý et al. (2011) and Řoutil et al. (2012).

4.3. Results − load−displacement curves

Two types of results from the conducted simulations are utilized in the subsequent analysis. One group is represented by the load−displacement diagrams that shall simulate the corresponding experimental

Tab. 2: Selected variants of the material model parameters

Concrete	E	f_t	G_f	l_{ch}	Note
	GPa	MPa	Jm^{-2}	m	
C0	32.29	2.56800	64.2	0.31435	${}^0l_{ch}$
C4+	32.29	1.81585	128.4	1.25740	$4\times{}^0l_{ch}$
C16+	32.29	1.28400	256.8	5.02960	$16\times{}^0l_{ch}$

records. Due to the wedge mechanism in the area where the load was imposed, special treatment of the recorded quantities must be taken into account. As is obvious from Fig. 4 left, the imposed load P is transferred from the loading wedge to the roller bearings as forces P^{P} and P^{L} on the interface between the wedge and the bearings on the right and left side, respectively. These forces are perpendicular to the side edge of the loading wedge (of angle α_w) and can be decomposed into horizontal splitting force P_{sp} and vertical force $P_v = P/2$.

The dependences of the forces on the displacements of their points of action are necessary for the determination of mechanical work, an energetic quantity, in the following analysis. Two alternatives of the dependences were considered: *i)* the load−displacement diagrams were drawn as functions of both the right and left reaction on the wedge−bearing interface, these being P^{P} and P^{L}, respectively, and the corresponding displacement of the roller bearings' axis on either side (determined as the vector composition of the horizontal and vertical displacement), *ii)* and as functions of both the horizontal splitting force P_{sp} on the mutual horizontal displacements of the roller bearings' axis and the vertical force P_v on the vertical roller bearings' axis displacement (in both the force and the vertical displacement case, the mean value from the right and left side was considered). The former and latter alternative is shown for selected relative notch length simulations in the top and bottom row of Fig. 5, respectively. Simulated responses for both the reference (*V1*) and alternative (*V2*) variants of the geometric model and the reference (*C0*) and two adjusted (*C4+* and *C16+*) material sets are compared there. Results for the other relative notch lengths can be found in Holušová (2012).

4.4. Results − crack patterns

The other results relevant to the study are represented by the crack patterns from which the extent of the material failure is apparent. As is evident from Fig. 6, the failure around the groove corners does not develop in the case of the alternative model and so none of the energy flux from the external loading is aimed at the corner areas. Contrariwise, in the case of the reference model, significant failure takes place at these locations in direct relation to the size of the notch and characteristic length. The crack patterns correspond to a stage in the fracture process at peak load. Figs. 5 and 6 correspond

i) dependences of the right and left reactions on the wedge−roller bearing interface P^{P} and P^{L}, resp., on the resulting displacement of the roller bearing's axis on either side

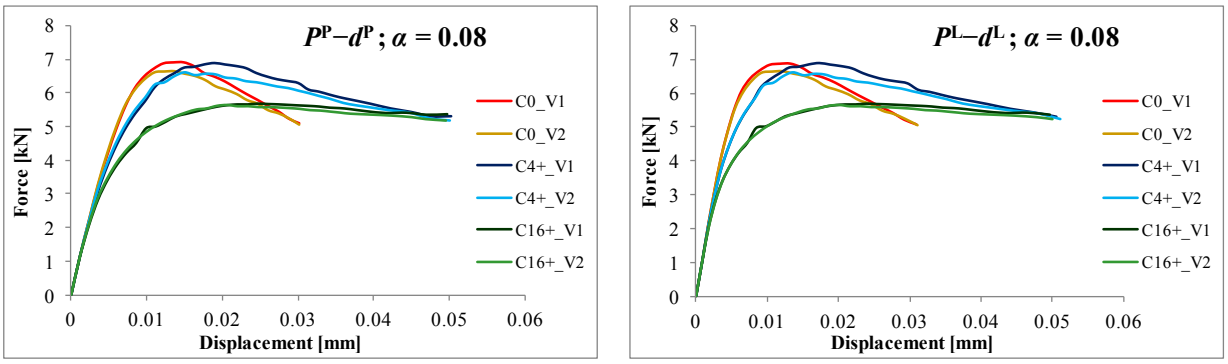

ii) dependences of the splitting and vertical force P_{sp} and P_v, resp., on the mutual horizontal and mean value of vertical displacement, resp., of the roller bearing's axis on either side

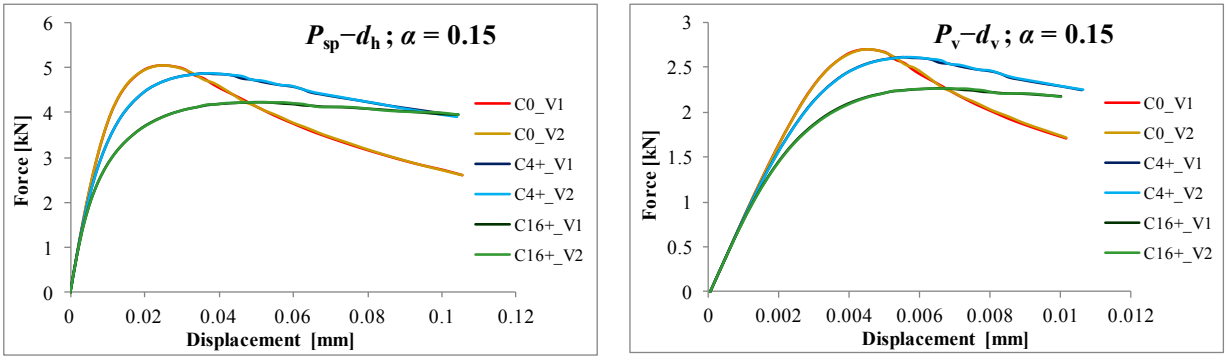

Fig. 5: Simulated load−displacement diagrams for selected relative notch lengths and selected material parameters sets

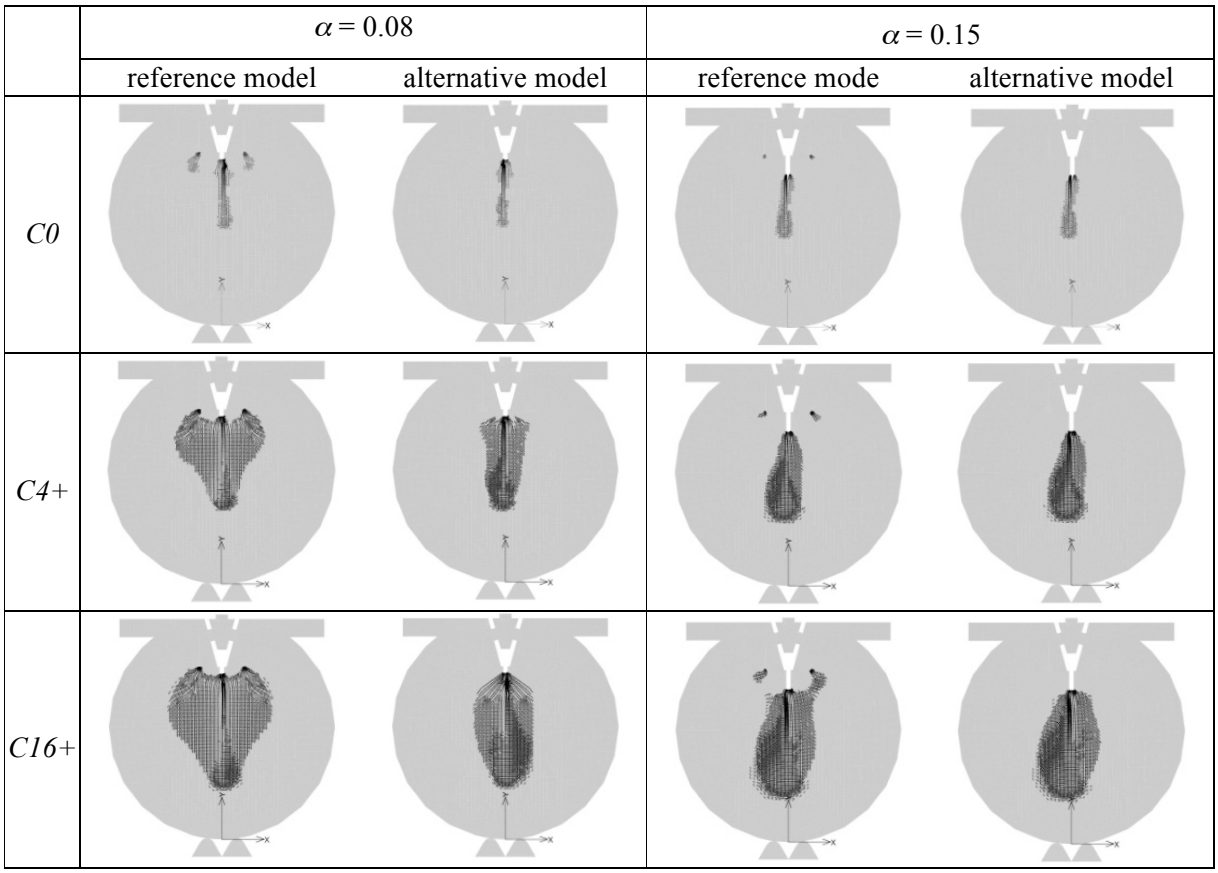

Fig. 6: Simulated crack patterns representing the extent of the material failure zone at the peak load stage of the load−displacement diagrams; the figures correspond to the loading curves in Fig. 5

well in showing the trend in the amount of energy needed for the fracture propagation around the groove corners; it is obvious from the differences (between model variants *V1* and *V2*) between the failure zone extents in Fig. 6 and between the areas under the loading curves in Fig. 5. Again, complete results for the whole of the study described here are presented in Holušová (2012).

4.5. Evaluation of the energy release for failures around the groove corners

As was discussed above, a difference exists in the extent of the zone of failure between the reference model (the real test) and the alternative model (the artificial variant). The difference corresponds to the difference in the load−displacement curves, which is particularly apparent near peak load and in a relatively short part after it. Therefore, in order to quantify the difference, work of fracture values were calculated from the load−displacement diagrams simulated for the *V1* and *V2* model variants.

The work of fracture W_f is calculated as

$$W_\mathrm{f} = W - U, \quad \text{where} \quad W = \int P \,\mathrm{d}d \quad \text{and} \quad U = \frac{1}{2} P d. \tag{2}$$

The integration was performed numerically using the trapezoidal rule. Actually, the value of work of fracture was not calculated from the whole load−displacement diagram but only from the portion up to the point where the curves for the *V1* and *V2* variants start to match. Considerable computational error accumulates at the tail of the simulated loading curve. Therefore, processing of the tail part of the curve was avoided. The absolute value of the amount of energy dissipated around the groove corners can then be estimated as

$$\Delta W_\mathrm{f} = {}^{V1}W_\mathrm{f} - {}^{V2}W_\mathrm{f}. \tag{3}$$

In order to relate the absolute amount of energy dissipation at the groove corners to the entire work of fracture value corresponding to the fracture propagated through the whole specimen ligament, the quantity $\overline{W_\mathrm{f}}$ was introduced. Due to the above-mentioned error at the load−displacement curve tail

$\overline{W_f}$ is estimated as a product of the area of the specimen ligament $A = (D - a_0)B$, where D is the specimen width, a_0 is the notch length and B is the specimen breadth, and the value of fracture energy G_f serving as the input to the FE calculations (see Tab. 2), i.e. $\overline{W_f} = G_f A$. Then, the relative amount of parasitic energy dissipation is calculated as

$$\omega_f = \Delta W_f / \overline{W_f}. \tag{4}$$

The quantities ΔW_f and ω_f were calculated for both types of load−displacement curve representation, i.e. the P^P–d^P, P^L–d^L and P_{sp}–d_h, P_v–d_v curves, respectively.

5. Discussion of results

The absolute and relative quantities representing the energy release around the corners of the groove for inserting the loading platens into the WST specimen for the three material sets (*C0*, *C4+* and *C16+*) and several considered notch lengths are shown in graphs in Fig. 7. The trends of the curves obviously correspond to the graphical representations of the failure depicted in Fig. 6.

The amount of parasitic energy dissipation decreases with increasing notch length, and for relative notch lengths around 0.25 it can be neglected. Facts resulting from the comparison of the absolute and relative energy dissipation are worth noticing. Whilst the absolute dissipation is higher for larger characteristic lengths (and visually agrees with the failure extents given by crack patterns), its relative value slightly decreases with increasing brittleness (i.e. decreasing l_{ch}). This fact is not obvious from a basic comparison of the load−displacement curves and crack patterns.

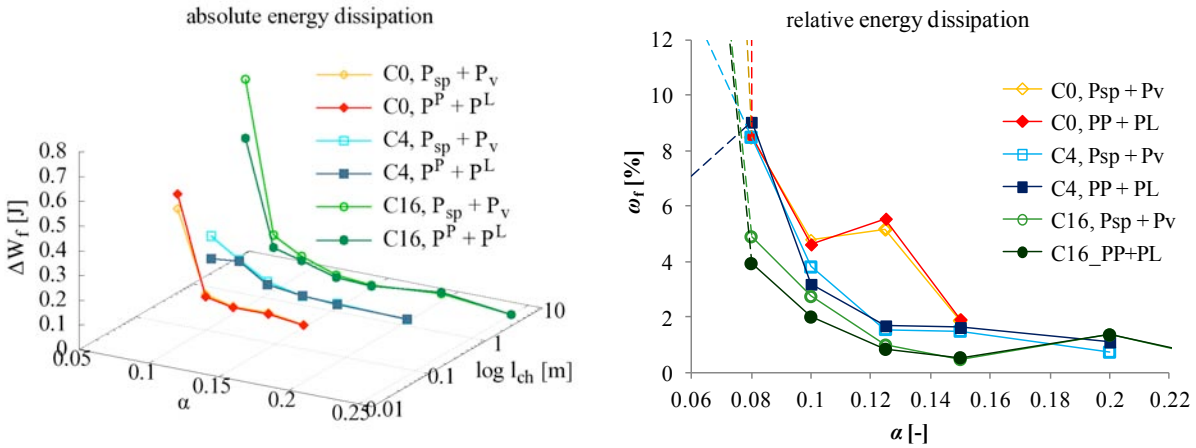

Fig. 7: The amount of absolute and relative energy dissipation around groove corners as a function of the relative notch length for three levels of brittleness of cementitious composite

This analysis is supplemented by an estimation of the minimal length of the notch in Holušová (2012). This is the minimal notch length that must be cut in the test specimen in order to obtain the major fracture propagation from the notch tip and not the groove corner. It is intended that this study will be supplemented with more potential variants of specimen shapes, sizes and boundary conditions/testing fixtures to provide a tool (recommendation) for experimental testing resulting in more accurate estimates of the fracture-mechanical parameters of tested materials.

6. Conclusions

This paper focuses on the analysis of failure in the cylinder-shaped WST specimens used for determination of the fracture-mechanical parameters of quasi-brittle materials. The amount of parasitic energy dissipated outside of the desired volume of the specimen is evaluated based on the numerically simulated responses of fracture tests. This amount of energy causes overestimation of the determined fracture-mechanical parameters, particularly fracture energy. The main conclusions from this study on the particular case of the size and shape of the specimen can be summarized in the following points:

- The amount of energy dissipated additionally around the groove corners decreases with increasing notch length; for short notches (α less than 0.1) it can take a proportion of the entire dissipated energy ranging from 3 to 10 %. For notches with a relative length greater than approx. 0.25 the effect becomes negligible.
- An increase in the absolute amount and a slight decrease in the relative amount of parasitic energy dissipation with increasing characteristic length are observed; an extension of this study in this respect is worth considering. However, it seems that for a common range of (quasi-)brittleness of cementitious composites the previous item holds true.

Verification of these results via another simulation method as well as experimental validation of the basic conclusions of this study is planned for future research.

Acknowledgement

This outcome has been achieved with the financial support of the Czech Scientific Foundation, project No. GA CR P105/11/1551.

References

Brühwiler, E. & Wittmann, F.H. (1990) The wedge splitting test, a new method of performing stable fracture mechanics test, *Engineering Fracture Mechanics*, 35, pp. 117-125.

Červenka, V. et al. (2005) *ATENA Program Documentation, Theory and User manual*. Prague: Cervenka Consulting.

Holušová, T. (2012) *Analýza napjatosti a porušení ve zkušebních tělesech používaných pro určování lomově-mechanických parametrů kvazikřehkých materiálů. Diploma Thesise.* Brno: BUT Brno, Faculty of Civil Engineering, Institute of Structural Mechanics, 74 p., 20 p. appendix (in Czech).

Holušová, T. & Veselý, V. (2011) Numerické simulace porušení v betonových válcových tělesech při zkoušce štípáním klínem. In: Proc. of *Víceúrovňový design pokrokových materiálů 2011* (I. Dlouhý, J. Švejcar & M. Šob eds.), Brno, 1st–2nd December 2011. Institute of Physics of Materials AV CR, v. v. i., pp. 185-192 (in Czech).

Linsbauer, H.N. & Tschegg, E.K. (1986) Fracture energy determination of concrete with cube-shaped specimens, *Zement und Beton*, 31, pp. 38-40.

RILEM Report 5 (1991) *Fracture Mechanics Test Methods for Concrete*, S.P. Shah, A. Carpinteri (Eds.), Hall, London.

Řoutil, L., Veselý, V. & Seitl, S. (2010a) Numerical study of wedge-splitting test on concrete specimens, In: *Proc. of Applied mechanics 2010* (J. Blekta ed.), Jablonec nad Nisou, 19th–22nd April 2010. Technical University of Liberec, pp. 107-110.

Řoutil, L., Veselý, V., Seitl, S. & Klusák, J. (2010b) Posouzení geometrie zkušebního tělesa pro WST kvazikřehkých kompozitů: Numerická studie. In: Proc. of *Křehký lom 2010, (Design a porušování material)* (I. Dlouhý ed.), Brno, 4th November 2010. Institute of Physics of Materials AS CR, v. v. i., pp. 201-212 (in Czech).

Řoutil, L., Veselý, V. & Seitl, S. (2011a) Wedge splitting test of quasi-brittle cylinder-shaped specimen: Numerical study on minimal notch length. In: *Proc. of Applied Mechanics 2011* (L. Náhlík, M. Zouhar, M. Ševčík, S. Seitl & Z. Majer eds.)., Velké Bílovice, 18th–20th April 2011 IPM AS CR, v. v. i., pp. 179-182.

Řoutil, L., Veselý, V., Seitl, S. & Klusák, J. (2011b) Optimal proportions of wedge splitting test specimen for testing of various cement based composites. In: Proc. of *1st Interquadrennial ICF Conference in Middle East and Africa* (CD) (A.-M. El-Batahgy & M. Waly eds.), Luxor, Egypt, November 14–17, 2011, pp. 457-465.

Řoutil, L., Veselý, V. & Seitl, S. (2012) Fracture analysis of cube- and cylinder-shaped WST specimens made of cementitious composites with various characteristic length. *Key Engineering Materials*, Vols. 488–489, pp. 533-536.

Seitl, S., Veselý, V. & Řoutil, L. (2011) Two-parameter fracture mechanical analysis of a near-crack-tip stress field in wedge splitting test specimens. *Computers and Structures*, 89, pp. 1852-1858.

Veselý, V., Řoutil, L. & Seitl, S. (2011) Wedge-splitting test – determination of minimal starting notch length for various cement based composites. Part I: Cohesive crack modelling. *Key Engineering Materials*, Vols. 452-453, pp. 77-80.

Veselý, V., Šestáková, L. & Seitl, S. (2012) Influence of boundary conditions on higher order terms of near-crack-tip stress field in a WST specimen. *Key Engineering Materials*, Vols. 488–489, pp. 399-402.